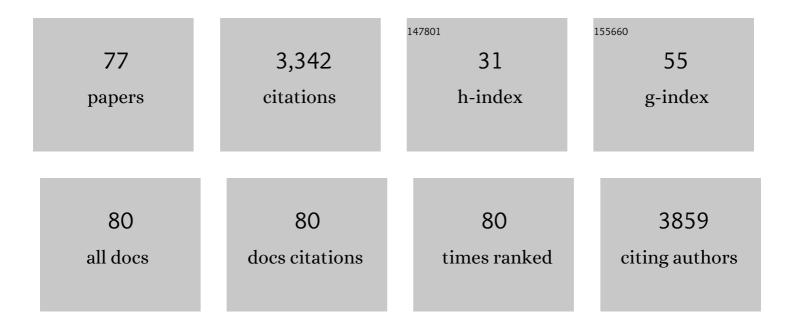
Xun Cao

List of Publications by Year in descending order

Source: https://exaly.com/author-pdf/5283781/publications.pdf Version: 2024-02-01



YUN CAO

#	Article	IF	CITATIONS
1	Interpenetrating interfaces for efficient perovskite solar cells with high operational stability and mechanical robustness. Nature Communications, 2021, 12, 973.	12.8	189
2	Ultrafine Metal Nanoparticles/Nâ€Doped Porous Carbon Hybrids Coated on Carbon Fibers as Flexible and Binderâ€Free Water Splitting Catalysts. Advanced Energy Materials, 2017, 7, 1700220.	19.5	156
3	Van der Waals negative capacitance transistors. Nature Communications, 2019, 10, 3037.	12.8	144
4	Exploring the impact of atomic lattice deformation on oxygen evolution reactions based on a sub-5 nm pure face-centred cubic high-entropy alloy electrocatalyst. Journal of Materials Chemistry A, 2020, 8, 11938-11947.	10.3	137
5	Recent advances in VO ₂ -based thermochromic composites for smart windows. Journal of Materials Chemistry C, 2018, 6, 1903-1919.	5.5	136
6	Nanoporous Thermochromic VO ₂ (M) Thin Films: Controlled Porosity, Largely Enhanced Luminous Transmittance and Solar Modulating Ability. Langmuir, 2014, 30, 1710-1715.	3.5	134
7	Facile and Low-Temperature Fabrication of Thermochromic Cr ₂ O ₃ /VO ₂ Smart Coatings: Enhanced Solar Modulation Ability, High Luminous Transmittance and UV-Shielding Function. ACS Applied Materials & Interfaces, 2017, 9, 26029-26037.	8.0	120
8	Phase-controllable growth of ultrathin 2D magnetic FeTe crystals. Nature Communications, 2020, 11, 3729.	12.8	120
9	Terbium-Doped VO ₂ Thin Films: Reduced Phase Transition Temperature and Largely Enhanced Luminous Transmittance. Langmuir, 2016, 32, 759-764.	3.5	112
10	Review on thermochromic vanadium dioxide based smart coatings: from lab to commercial application. Advances in Manufacturing, 2018, 6, 1-19.	6.1	107
11	Spatially Resolved Dynamically Reconfigurable Multilevel Control of Thermal Emission. Laser and Photonics Reviews, 2020, 14, 1900162.	8.7	103
12	High Performance and Enhanced Durability of Thermochromic Films Using VO ₂ @ZnO Core–Shell Nanoparticles. ACS Applied Materials & Interfaces, 2017, 9, 27784-27791.	8.0	102
13	Confining Tiny MoO ₂ Clusters into Reduced Graphene Oxide for Highly Efficient Low Frequency Microwave Absorption. Small, 2020, 16, e2001686.	10.0	87
14	Challenges and Opportunities toward Real Application of VO2-Based Smart Glazing. Matter, 2020, 2, 862-881.	10.0	83
15	Phase engineering of Cr5Te8 with colossal anomalous Hall effect. Nature Electronics, 2022, 5, 224-232.	26.0	68
16	Reversible Al Metal Anodes Enabled by Amorphization for Aqueous Aluminum Batteries. Journal of the American Chemical Society, 2022, 144, 11444-11455.	13.7	63
17	Self-assembled Cu-Ni bimetal oxide 3D in-plane epitaxial structures for highly efficient oxygen evolution reaction. Applied Catalysis B: Environmental, 2019, 244, 56-62.	20.2	62
18	Oxygen vacancy mediated bismuth stannate ultra-small nanoparticle towards photocatalytic CO2-to-CO conversion. Applied Catalysis B: Environmental, 2020, 276, 119156.	20.2	59

Χυν ζαο

#	Article	IF	CITATIONS
19	Rational design of intertwined carbon nanotubes threaded porous CoP@carbon nanocubes as anode with superior lithium storage. Carbon, 2019, 142, 269-277.	10.3	58
20	Nanostructured Metal–Organic Conjugated Coordination Polymers with Ligand Tailoring for Superior Rechargeable Energy Storage. Small, 2019, 15, e1903188.	10.0	57
21	Application-oriented VO2 thermochromic coatings with composite structures: Optimized optical performance and robust fatigue properties. Solar Energy Materials and Solar Cells, 2019, 189, 138-148.	6.2	57
22	Mitigating Deterioration of Vanadium Dioxide Thermochromic Films by Interfacial Encapsulation. Matter, 2019, 1, 734-744.	10.0	55
23	Effects of V2O3 buffer layers on sputtered VO2 smart windows: Improved thermochromic properties, tunable width of hysteresis loops and enhanced durability. Applied Surface Science, 2018, 441, 764-772.	6.1	53
24	Self-Template Synthesis of Nanoporous VO ₂ -Based Films: Localized Surface Plasmon Resonance and Enhanced Optical Performance for Solar Glazing Application. ACS Applied Materials & Interfaces, 2019, 11, 22692-22702.	8.0	53
25	High thermoelectric performance enabled by convergence of nested conduction bands in Pb7Bi4Se13 with low thermal conductivity. Nature Communications, 2021, 12, 4793.	12.8	53
26	Nanostructured CuO/C Hollow Shell@3D Copper Dendrites as a Highly Efficient Electrocatalyst for Oxygen Evolution Reaction. ACS Applied Materials & amp; Interfaces, 2018, 10, 23807-23812.	8.0	49
27	The synergistic catalysis on Co nanoparticles and CoNx sites of aniline-modified ZIF derived Co@NCs for oxidative esterification of HMF. Chinese Chemical Letters, 2021, 32, 685-690.	9.0	47
28	The Self-Passivation Mechanism in Degradation of BiVO4 Photoanode. IScience, 2019, 19, 976-985.	4.1	40
29	Conductivity Modulation of 3Dâ€Printed Shellular Electrodes through Embedding Nanocrystalline Intermetallics into Amorphous Matrix for Ultrahighâ€Current Oxygen Evolution. Advanced Energy Materials, 2021, 11, 2100968.	19.5	40
30	High Thermoelectric Performance through Crystal Symmetry Enhancement in Triply Doped Diamondoid Compound Cu ₂ SnSe ₃ . Advanced Energy Materials, 2021, 11, 2100661.	19.5	39
31	Superior Li-ion storage of VS ₄ nanowires anchored on reduced graphene. Nanoscale, 2019, 11, 9556-9562.	5.6	35
32	Highly anisotropic thermoelectric properties of black phosphorus crystals. 2D Materials, 2019, 6, 045009.	4.4	33
33	Atomically Dispersed Intrinsic Hollow Sites of <i>M</i> â€ <i>M</i> ₁ â€ <i>M</i> (<i>M</i> ₁ Â= Pt, Ir; <i>M</i> Â= Fe, Co, Ni, Cu, Pt, Ir) on FeCoNiCuPtIr Nanocrystals Enabling Rapid Water Redox. Advanced Functional Materials, 2022, 32, .	14.9	33
34	Confinement of single polyoxometalate clusters in molecular-scale cages for improved flexible solid-state supercapacitors. Nanoscale, 2020, 12, 11887-11898.	5.6	31
35	Innovative development on a p-type delafossite CuCrO2 nanoparticles based triethylamine sensor. Sensors and Actuators B: Chemical, 2020, 324, 128743.	7.8	29
36	Highly Enhanced Thermochromic Performance of VO2 Film Using "Movable―Antireflective Coatings. ACS Applied Materials & Interfaces, 2019, 11, 4712-4718.	8.0	28

Xun Cao

#	Article	IF	CITATIONS
37	How to properly evaluate and compare the thermochromic performance of VO ₂ -based smart coatings. Journal of Materials Chemistry A, 2019, 7, 24164-24172.	10.3	28
38	Development of polyoxometalate-anchored 3D hybrid hydrogel for high-performance flexible pseudo-solid-state supercapacitor. Electrochimica Acta, 2020, 329, 135181.	5.2	28
39	A plasmonic non-stoichiometric WO _{3â^'x} homojunction with stabilizing surface plasmonic resonance for selective photochromic modulation. Chemical Communications, 2018, 54, 5241-5244.	4.1	26
40	Solution-based fabrication of VO ₂ (M) nanoparticles via lyophilisation. RSC Advances, 2015, 5, 25669-25675.	3.6	24
41	Highly flexible interconnected Li+ ion-sieve porous hydrogels with self-regulating nanonetwork structure for marine lithium recovery. Chemical Engineering Journal, 2022, 445, 136780.	12.7	24
42	Microwave Absorption: Confining Tiny MoO ₂ Clusters into Reduced Graphene Oxide for Highly Efficient Low Frequency Microwave Absorption (Small 30/2020). Small, 2020, 16, 2070168.	10.0	23
43	Dual-Nitrogen-Doped Carbon Decorated on Na ₃ V ₂ (PO ₄) ₃ to Stabilize the Intercalation of Three Sodium Ions. ACS Applied Energy Materials, 2020, 3, 6870-6879.	5.1	23
44	Electrons-Donating Derived Dual-Resistant Crust of VO ₂ Nano-Particles via Ascorbic Acid Treatment for Highly Stable Smart Windows Applications. ACS Applied Materials & Interfaces, 2019, 11, 41229-41237.	8.0	22
45	Extraordinary catalysis induced by titanium foil cathode plasma for degradation of water pollutant. Chemosphere, 2019, 214, 341-348.	8.2	21
46	Porous cobalt@N-doped carbon derived from chitosan for oxidative esterification of 5-Hydroxymethylfurfural: The roles of zinc in the synthetic and catalytic process. Molecular Catalysis, 2020, 482, 110695.	2.0	21
47	Broadband thermochromic VO 2 -based composite film with ultra-high solar modulation ability. Materials Letters, 2018, 222, 62-65.	2.6	20
48	Ordered distributed nickel sulfide nanoparticles across graphite nanosheets for efficient oxygen evolution reaction electrocatalyst. International Journal of Hydrogen Energy, 2019, 44, 1544-1554.	7.1	20
49	Co-synthesis of CuO-ZnO nanoflowers by low voltage liquid plasma discharge with brass electrode. Journal of Alloys and Compounds, 2019, 773, 762-769.	5.5	19
50	Mechanically Durable Memristor Arrays Based on a Discrete Structure Design. Advanced Materials, 2022, 34, e2106212.	21.0	19
51	Transmittance change with thickness for polycrystalline VO2 films deposited at room temperature. Journal of Alloys and Compounds, 2019, 791, 648-654.	5.5	18
52	Molecular-scale cage-confinement pyrolysis route to size-controlled molybdenum carbide nanoparticles for electrochemical sensor. Biosensors and Bioelectronics, 2020, 165, 112373.	10.1	17
53	Sputtering Flexible VO ₂ Films for Effective Thermal Modulation. ACS Applied Materials & Interfaces, 2022, 14, 28105-28113.	8.0	17
54	The Electrochemical Response of Single Crystalline Copper Nanowires to Atmospheric Air and Aqueous Solution. Small, 2017, 13, 1603411.	10.0	15

Χυν ζαο

#	Article	IF	CITATIONS
55	Chemical Vapor Deposition of Superconducting FeTe _{1–<i>x</i>} Se _{<i>x</i>} Nanosheets. Nano Letters, 2021, 21, 5338-5344.	9.1	15
56	Multifunctional Flexible Vanadium Dioxide Films. Accounts of Materials Research, 2021, 2, 714-725.	11.7	14
57	Highly Strained Au Nanoparticles for Improved Electrocatalysis of Ethanol Oxidation Reaction. Journal of Physical Chemistry Letters, 2020, 11, 3005-3013.	4.6	12
58	Catalysis of Au nano-pyramids formed across the surfaces of ordered Au nano-ring arrays. Journal of Catalysis, 2019, 377, 389-399.	6.2	11
59	Tunable low-dimensional self-assembly of H-shaped bichromophoric perylenediimide Gemini in solution. Nanoscale, 2020, 12, 3058-3067.	5.6	11
60	Strained Ultralong Silver Nanowires for Enhanced Electrocatalytic Oxygen Reduction Reaction in Alkaline Medium. Journal of Physical Chemistry Letters, 2021, 12, 2029-2035.	4.6	10
61	A three-dimensional porous MoS ₂ –PVP aerogel as a highly efficient and recyclable sorbent for oils and organic solvents. Materials Advances, 2020, 1, 760-766.	5.4	9
62	Growth of Lattice Coherent Co 9 S 8 /Co 3 O 4 Nanoâ€Heterostructure for Maximizing the Catalysis of Coâ€Based Composites. ChemCatChem, 2020, 12, 2431-2435.	3.7	9
63	Epitaxial Bi9Ti3Fe5O27 thin films: a new type of layer-structure room-temperature multiferroic. Journal of Materials Chemistry C, 2017, 5, 7720-7725.	5.5	8
64	Janus-like particles prepared through partial UV irradiation at the water/oil interface and their encapsulation capabilities. Colloids and Surfaces A: Physicochemical and Engineering Aspects, 2020, 589, 124460.	4.7	8
65	One-step fabrication of Cu2O-Cu catalytic electrodes with regular porous array by ultra-fast laser scanning. Journal of Alloys and Compounds, 2022, 900, 163455.	5.5	8
66	Design of Hierarchical Oxideâ€Carbon Nanostructures for Trifunctional Electrocatalytic Applications. Advanced Materials Interfaces, 2022, 9, .	3.7	8
67	Facile synthesis of hydrated magnesium vanadium bronze σ-Mg0.25V2O5·H2O as a novel cathode material for lithium-ion batteries. Journal of Alloys and Compounds, 2019, 777, 931-938.	5.5	7
68	Decomposition behavior in the early-stage oxidation of Sm2Co17-type magnets. Scripta Materialia, 2021, 200, 113911.	5.2	7
69	Atomic-scale oxidation of a Sm2Co17-type magnet. Acta Materialia, 2021, 220, 117343.	7.9	6
70	Metal-organic framework derived Co ₃ Se ₄ @Nitrogen-doped porous carbon as a high-performance anode material for lithium ion batteries. Nanotechnology, 2020, 31, 215602.	2.6	6
71	Solid-Ionic Memory in a van der Waals Heterostructure. ACS Nano, 2022, 16, 221-231.	14.6	6
72	Bifunctional copper cathode induced oxidation of glycerol with liquid plasma discharge. Separation and Purification Technology, 2019, 220, 328-333.	7.9	5

Xun Cao

#	Article	IF	CITATIONS
73	Unraveling the effects of anions in NixAy@CC (A=O, S, P) on Li-sulfur batteries. Materials Today Nano, 2021, 13, 100106.	4.6	5
74	Twinning enhanced electrical conductivity and surface activity of nanostructured CuCrO2 gas sensor. Sensors and Actuators B: Chemical, 2021, 338, 129845.	7.8	4
75	Bioactive CaTiO3 film prepared on the biomedical porous Ti–15Mo alloy by one-step hydrothermal treatment. Journal of Materials Research and Technology, 2021, 14, 202-209.	5.8	4
76	Flexible Au micro-array electrode with atomic-scale Au thin film for enhanced ethanol oxidation reaction. Nano Research, 2021, 14, 311-319.	10.4	3
77	Zinc Ferrite Nanoparticles: Simple Synthesis via Lyophilisation and Electrochemical Application as Glucose Biosensor. Nano Express, 0, , .	2.4	2